



# Influence of Nanocarrier Type on the Drug Delivery Aspects of Docetaxel: Empirical Evidences

Saad M. Alshahrani<sup>1</sup> · Nagarani Thotakura<sup>2</sup> · Saurabh Sharma<sup>3,4</sup> · Sheikh Shahnawaz Quadir<sup>2</sup> · Nishtha Chaurawal<sup>2</sup> · Sumit Sharma<sup>5</sup> · Deepak Chitkara<sup>4</sup> · Kaisar Raza<sup>2</sup>

Accepted: 3 August 2022 / Published online: 11 August 2022

© The Author(s), under exclusive licence to Springer Science+Business Media, LLC, part of Springer Nature 2022

## Abstract

**Purpose** Docetaxel (DTX) is one of the anti-neoplastic drugs widely employed in breast cancer management. Along with advantages, several challenges are associated with administering the BCS class IV drugs like DTX. Looking into the promises of various nanotechnology-based drug delivery systems, it was envisioned to explore the influence of carrier type on the drug delivery outcome for this anticancer agent.

**Methods** In the present study, docetaxel was encapsulated into solid lipid nanoparticles, nano-lipoidal carriers, liposomes, niosomes, and microemulsion systems and the various systems were characterized. The carriers were also evaluated for drug release profile, anticancer activity on cell lines, apoptosis assays, and hemocompatibility.

**Results** The developed nano-formulations were found to offer a spatiotemporal pattern of drug release. There was a substantial enhancement in the cytotoxicity of the drug against the cancer cells. It was vouched by the flow-cytometry assay and MTT-cytotoxicity studies. The developed systems were found to be compatible with the erythrocytes vis-à-vis the plain drug.

**Conclusion** The study encompassing the drug loading and drug release capabilities of a BCS class IV drug, offering scientific evidence for better efficacy and safety coupled with plasma protein binding insights, provides a platform to select appropriate nanocarrier out of the plethora of options.

**Keywords** Solid lipid nanoparticles · Nano-lipoidal carriers · Liposomes · Microemulsion · Niosomes

## Introduction

Delivery of drug molecules of more significant size generally poses a major challenge of poor solubility, which indirectly affects the absorption and bioavailability of the drug. The drug delivery also results in in vivo instability, dose-dependent adverse effects, and issues related to the targeted drug delivery [1]. Therefore, the advent of novel drug delivery systems resolved these challenges [2, 3]. The

developments in nanotechnology have played a vital role in designing specialized novel drug delivery systems, which possess drug targeting potential and controlled drug release characteristics [4].

In between physical and biological sciences, nanotechnology acts as a connecting bridge with the advent of nanotechnology-based drug delivery systems and nanomedicine. For practical purposes in pharmaceutical sciences, nanomaterials are materials that fall in the range of 1–1000 nm [5]. These nano-sized particles inherit specific unique structural, chemical, and biological properties. The most commonly used nanotechnologies in medicine involve tissue engineering, microfluidics, biosensors, micro assays, and drug delivery [6]. In the recent era, nanomedicine came into the limelight, as the nanocarriers can encapsulate or attach the drug molecules and deliver the active pharmaceutical ingredients at the target site in a controlled manner [7]. Owing to their nanostructures, these systems are reported to penetrate the tissues quickly. These systems also help in enhancing the cellular uptake, which is a

## Highlights

- The type of nanocarrier influences the overall outcome of the drug delivery systems.
- Most of the nanocarriers controlled the release of docetaxel.
- All the nanocarriers were biocompatible.
- Liposomes offered substantial drug entrapment, and microemulsion showed maximum drug loading.
- The best anticancer outcomes were from the microemulsion

✉ Kaisar Raza  
drkaisar@curaj.ac.in; razakaisar\_pharma@yahoo.co.in

Extended author information available on the last page of the article

testimony to the targeted action at the diseased site [8]. Due to targeted action at the site of infection, there is a propensity to reduce adverse effects and the plethora of chances and promises of improved efficacy [9]. Therefore, drug release can be achieved at a predetermined rate [10]. The share of nanotechnology-based drug delivery products is escalating in the market. There are various lipid-based, polymer-based, mineral-based, and carbon-based nanocarriers, which encompass polymeric micelles, nanostructured lipidic carriers (NLCs), mixed micelles, nanoparticles, niosomes, liposomes, solid lipid nanoparticles (SLNs), and micro and nanoemulsions [2, 3, 11].

Although the chemotherapeutic drug, docetaxel (DTX), is a promising agent for breast cancer management, still there is massive scope for improvement due to the various concerns [12]. The primary concern is poor oral bioavailability, which is reported to be < 10%, generally ascribable to the first-pass metabolism. The second major challenge is the constraint of aqueous insolubility [13]. Due to the concerns of the poor bioavailability, the frequent route of administration is the parenteral route. It requires vast amounts of surfactants, which generally result in unwanted effects like tissue necrosis, neutropenia, hypersensitivity, and many other side effects [14]. Peripheral neuropathy, alopecia, anemia, myalgias, fluid retention, anorexia, hypersensitivity reactions, mucositis, skin, and nail toxicity are the common side effects of DTX [15, 16]. In an attempt to explore the effect of nanocarriers like SLNs, NLCs, liposomes, niosomes, and microemulsions on the overall performance of DTX, it was envisioned to entrap DTX in the selected nanocarriers and evaluate its performance using breast cancer cell lines. This study will add more understanding to the delivery aspects of these nanocarriers, especially for a drug that is quite problematic and belongs to the biopharmaceutical classification system (BCS) class IV category. Till date, no such study has been reported where all these carrier systems are being compared for the delivery of DTX.

## Materials and Methods

### Materials Used

Docetaxel and unsaturated phospholipid, Phospholipon 90 G, were obtained as gift samples from M/s Fresenius Kabi Oncology Ltd., Gurgaon, Haryana, India, and M/s IPCA Labs, Mumbai, respectively. 3-(4,5-dimethylthiazol-2-yl)-2,5-diphenyltetrazolium bromide (abbreviated as MTT) and  $\alpha$ -tocopheryl acetate isopropyl myristate were obtained from M/s Sigma–Aldrich. In contrast, ethanol, HPLC-acetonitrile (ACN), HPLC-water, stearic acid, Tween-80, and Span-80 were purchased from M/s Spectrochem Co., Ltd. All chemicals for the buffered solutions and isopropyl myristate

(IPM) were supplied by M/s CDH Co. Ltd. The source of dialysis membrane with a molecular cut-off of 12 kDa was M/s Himedia laboratories Co. Ltd. Cell line studies were performed at the Department of Pharmacy, BITS, Pilani, Rajasthan, India. The study used in-house distilled water, and the reagents/chemicals were used as provided by the respective vendor without any further purification.

### Preparation of NLCs

The standard microemulsification and subsequent dispersion method were employed to develop DTX-loaded and blank NLCs, using stearic acid as the solid lipid and  $\alpha$ -tocopheryl acetate as the liquid lipid component mass ratio of 5:1. Due to the meritorious features of phospholipids, Phospholipid 90 G was employed in the formulation ([11, 17, 18]. Initially, stearic acid (75 mg) was melted at 70 °C in a beaker to which DTX (10 mg) was added along with  $\alpha$ -tocopheryl acetate (15 mg) and Tween-80 (3 g) with continuous stirring. Separately, phospholipid (15 mg) was placed in 10 mL of water, maintained at 70 °C and dispersed properly till a milky dispersion was formed. The dispersion of the second beaker was added into the first one in a streamlined manner, with constant stirring of 100 rpm. The obtained hot and transparent emulsion was plunged into 10 mL of ice-cold water, followed by continuous stirring at 1000 rpm for 30 min. The resultant milky dispersion of the drug-loaded NLCs (DTX-NLCs) was adequately stored for further use. The blank formulation was also prepared using the same method without the drug [19].

### Preparation of SLNs

For the development of SLNs, initially in a beaker, stearic acid (90 mg) was melted, and DTX (10 mg) was added, followed by Tween-80 (3 g) at a temperature of 70 °C. In the second beaker, 15 mg of phospholipid dispersion was prepared using distilled water (q.s. to 10 mL) at the same temperature as the initial one. The dispersion of the second beaker was slowly poured into the first beaker with continuous stirring. A yellow colored hot and transparent microemulsion was formed. The hot microemulsion was added in a streamlined manner to 10 mL water, maintained at 4 °C, with continuous stirring. The obtained dispersion of the drug-loaded SLNs (DTX-SLNs) was stirred for 30 min and stored at ambient conditions. The blank formulation was also prepared analogously without drug use [20].

### Preparation of Liposomes

Liposomes were prepared using the ethanol injection method. Both the phospholipid and drug, in the mass ratio of 10:1, amounting to a total lipid content of 110 mg, were

dissolved in 1 mL of ethanol. The resulting solution was streamlined to distilled water (9 mL) with constant stirring. The obtained liposomal formulation (DTX-LP) was stored at proper conditions. The blank formulation was prepared using the same method without the drug [21].

### Preparation of Niosomes

The ethanol injection method was employed for the niosomal preparation. Span-80 and DTX in the mass ratio of 10:1, amounting to a total weight of 110 mg, were added to a test tube. Ethanol, 1 mL, was added to dissolve the contents using a vortex mixer. The ethanolic solution was poured drop-wise into a beaker containing distilled water with continuous stirring. The final volume was made up to 10 mL using distilled water. The resultant niosomal formulation (DTX-NIO) was stored for further use. The blank formulation was prepared using the same method without the drug [22].

### Preparation of Microemulsion

Isopropyl myristate (IPM) (1 mL) was mixed with Tween-80 (1 g) and stirred to dissolve 10 mg of DTX. Separately, phospholipid (100 mg) was dispersed in distilled water (q.s. to 10 mL). At a slow rate, phospholipid dispersion was mixed with the drug solution at room temperature with the help of constant stirring. This mixing resulted in the formulation of microemulsion (DTX-ME). The blank formulation was prepared using the same method without the drug [23]. Table 1 shows the composition of all the ingredients used in the preparation of nanoformulations. Table 1 Compositions involved in the preparation of the nanoformulations.

### Characterization of the Developed Nanocarriers

Drug loading and entrapment efficiency of the developed systems were determined using the dialysis bag method. In

this study, both the blank and drug-loaded formulations were packed into a dialysis bag with each 1 mL. These bags were dipped into beakers containing 50 mL methanol for a period of 2 h. The sample of 2 mL was collected and analyzed using the RP-HPLC method, which is mentioned in our previous papers [24].

All the formulations were observed for the micromeritic profile, including polydispersity index (PDI) and surface charge. The study was performed at Birla Institute of Technology and Science, Pilani (BITS Pilani), India, on Malvern Zetasizer. The reported reading was the average of the three runs [25]. The optical microscopy was performed for the liposomes and niosomes, and SLNs, NLCs, and microemulsion were observed under transmission electron microscope to confirm the nanocarrier formation.

### Evaluation Studies

#### In Vitro Drug Release Kinetics

Drug release studies were performed to know the rate and pattern of the drug release from the developed nanoparticulate systems. A very well-known dialysis method was employed for this purpose. This study was performed at both the physiological pH (pH 7.4) to understand the drug release characteristics in the plasma-like conditions and cancer cell pH (pH 5.6) to study the drug release characteristics in the cancer cytosol-like conditions. Pure drug (DTX) dispersions of 1 mg/mL in both the buffers, i.e., phosphate buffer solutions (PBS) of pH 5.6 and pH 7.4, were prepared and packed in two different dialysis bags. All the formulations were also packed in separate dialysis bags with drug equivalent to 1 mg/mL. These bags were separately dipped into the beakers containing 50 mL of pH 5.6 and 7.4, respectively. These beakers were continuously stirred at 50 rpm at  $37 \pm 0.5$  °C, and the sampling was done at the predetermined time intervals. Collected samples

**Table 1** Compositions involved in the preparation of the nanoformulations

Ingredients	NLCs	SLNs	Liposomes	Niosomes	Microemulsion
Stearic acid	75 mg	90 mg	—	—	—
Docetaxel	10 mg	10 mg	10 mg	10 mg	10 mg
$\alpha$ -Tocopheryl acetate	15 mg	—	—	—	—
Phospholipid	15 mg	15 mg	100 mg	—	100 mg
Tween-80	3 g	3 g	—	—	1 g
Ethanol	—	—	1 mL	1 mL	—
Span-80	—	—	—	100 mg	—
Isopropyl myristate	—	—	—	—	1 mL
Distilled water	10 mL	10 mL	10 mL	10 mL	10 mL

were analyzed using the RP-HPLC method. Obtained data were fitted into kinetic models like zero-order, first-order, Higuchi equation and Korsmeyer–Peppas equation to draw the inferences regarding the drug release pattern. Release flux values were calculated to know the release rate [26, 27]. All the results reported were the arithmetic mean of the three consecutive readings.

### Hemocompatibility Studies

The Institutional Ethical Committee of the Central University of Rajasthan, Rajasthan, India, approved this study protocol. This study was executed by collecting the blood sample (5 mL) from a healthy human volunteer into an EDTA-coated ampoule under strict medical supervision. To the collected blood, 5 mL of saline solution (standard) was added and subjected to centrifugation at a speed of 2000 rpm for 5 min. The lump of erythrocytes was harvested and washed 3–4 times with normal saline and resuspended in 10 mL of normal saline through decantation. Naïve drug (1 mg) along with the drug-loaded formulations, which contained drug equivalent to 1 mg of DTX, was added separately to 1 mL of the erythrocyte dispersion, followed by incubation of 1 h at 37 °C. The respective positive and negative controls were the RBCs suspended in normal saline and dispersed in distilled water. All the test and control samples were centrifuged for 5 min, and the clear supernatant was harvested. This supernatant was analyzed at a wavelength of 415 nm employing a UV–visible spectrophotometer [28].

### Protein Binding Studies

Protein binding studies were performed using the plasma collected from the human blood, which was left over from the hemocompatibility studies. Collected plasma was diluted using normal saline as per the requirement. To 1 mL of plasma, different volumes of the test samples (both DTX and the nanoformulations equivalent to DTX), i.e., 0.1, 0.2, 0.4, 0.6, 0.8, and 1 mL, were added. All the samples were kept for the overnight shaking, followed by centrifugation using ultracentrifuge at a speed of 24,000 rpm and temperature of 5 °C for 30 min. Equal amounts of supernatant and HPLC grade ACN were mixed and filtered through a 0.2 µ filter [29]. These samples were analyzed using RP-HPLC, whose method is reported elsewhere [30].

### Cell Viability Studies

The anticancer potential of the prepared nanoformulations was evaluated using the MDA-MB-231 cell lines.

The cells were inoculated and cultured in the well plates enriched with Dulbecco's Modified Eagle's Medium/Ham's F-12. The culture medium was supplemented with antibiotics (1% penicillin/streptomycin), fetal bovine serum (5%), and L-glutamine (1%). As per the standard protocol, the percentage of carbon dioxide was fixed at 5%. In the wells containing the cell cultures, DTX and the drug-loaded nanoformulations were added at a different concentration range and incubated for 24 h at 37 °C. Through centrifugation, formazan crystals were extracted after the scheduled addition of the MTT solution (10 µL of 2.5 mg/mL). These crystals were dissolved in 150 µL of dimethyl sulfoxide, and the optical density of the solution was measured by scanning at  $\lambda_{\text{max}}$  of 540 nm. The obtained results were further employed to determine the IC<sub>50</sub> values [17, 18].

### Apoptosis Assay

To study the apoptotic effect, cell lines with a density of  $1 \times 10^6$  cells per well were added to a six-well plate, seeded, and incubated for 24 h. The samples to be tested include plain DTX and all the other five drug-loaded nanoformulations in which the concentration of DTX was 50 nM. In these plates, media was removed, and the cells were rinsed with PBS of pH 7.4. They were trypsinized and followed by centrifugation at a speed of 1300 rpm for 3 min. The obtained cell pellet was suspended in sterilized cold PBS, pH 7.4 and recentrifuged for 5 min at 1700 rpm and 4 °C. After that, it was resuspended in Annexin V binding buffer [31]. The apoptosis was quantified using flow cytometry through the Annexin V-FITC conjugate and PI kit as per the supplier instructions. A preliminary analysis was performed to avoid background noise created by plain buffer and the untreated cells. Earlier to the post-acquisition analysis, autofluorescence of cells were eliminated from the view surface. The Annexin V FITC conjugate fluorescence was observed from the 525/40 bandpass filter, whereas it was a 610/20 bandpass filter for PI [32]. CytExpert 2.0 software (Cytotflex, M/s Beckman Coulter, USA) was used for the post-acquisition and data acquisition analysis [33].

### Statistical Analysis

Data obtained from various studies were subjected to statistical analysis to draw an inference. One-way ANOVA was employed for all the comparisons, as the same is the most prescribed for such data sets. The level of significance was mentioned at every necessary section. All the studies were repeated thrice unless

**Table 2** Drug loading and the entrapment efficiency of the developed drug-loaded nanoformulations

Nano formulations	% Drug loading	% Entrapment efficiency
DTX-SLNs	10.49 ± 0.89	84.98 ± 1.97
DTX-NLCs	13.10 ± 1.06	81.05 ± 2.01
DTX-LP	14.84 ± 1.24	88.47 ± 3.01
DTX-NIO	11.53 ± 1.18	85.32 ± 2.64
DTX-ME	13.63 ± 1.37	96.31 ± 2.89

mentioned and the data is represented in the form of mean ± SD.

## Results and Discussion

### Characterization Studies

The obtained % drug loading and % entrapment efficiency of the developed nanoformulations are displayed in Table 2. The high entrapment levels were observed, which may be inferred to the hydrophobic core of the nanocarrier, which attracts the hydrophobic DTX. Other than various forces like hydrogen bonding and Van der Waals interactions helped attain the loading of drug in the carrier system. Through these results, it can be envisioned that the hydrophobic carriers help in the better entrapment of the chemotherapeutic drugs belonging to BCS class IV [34].

Table 3 represents the results of the particle size, zeta potential, and PDI values of both blank and the drug-loaded nanoformulations. In all five formulations, it was observed that an enhancement in the particle size ensures

**Table 3** Values of micromeritic data and surface charge for both blank as well as drug-loaded nanoformulations

Nano formulations	Particle size (nm)	Zeta potential (mV)	PDI
Blank SLNs	101.93 ± 2.88	− 18.81 ± -0.63	0.320
DTX-SLNs	113.52 ± 1.15	− 29.23 ± -0.58	0.237
Blank NLCs	97.65 ± 1.73	− 16.25 ± -0.77	0.334
DTX-NLCs	106.39 ± 2.51	− 31.90 ± -0.86	0.174
Blank LP	87.53 ± 1.81	− 21.11 ± -0.94	0.484
DTX-LP	93.74 ± 1.07	− 25.94 ± -0.80	0.256
Blank NIO	76.49 ± 2.18	− 34.27 ± -0.73	0.371
DTX-NIO	103.32 ± 1.52	− 35.72 ± -0.55	0.224
Blank ME	88.91 ± 1.04	− 23.68 ± -0.65	0.387
DTX-ME	91.82 ± 0.97	− 31.26 ± -0.72	0.198

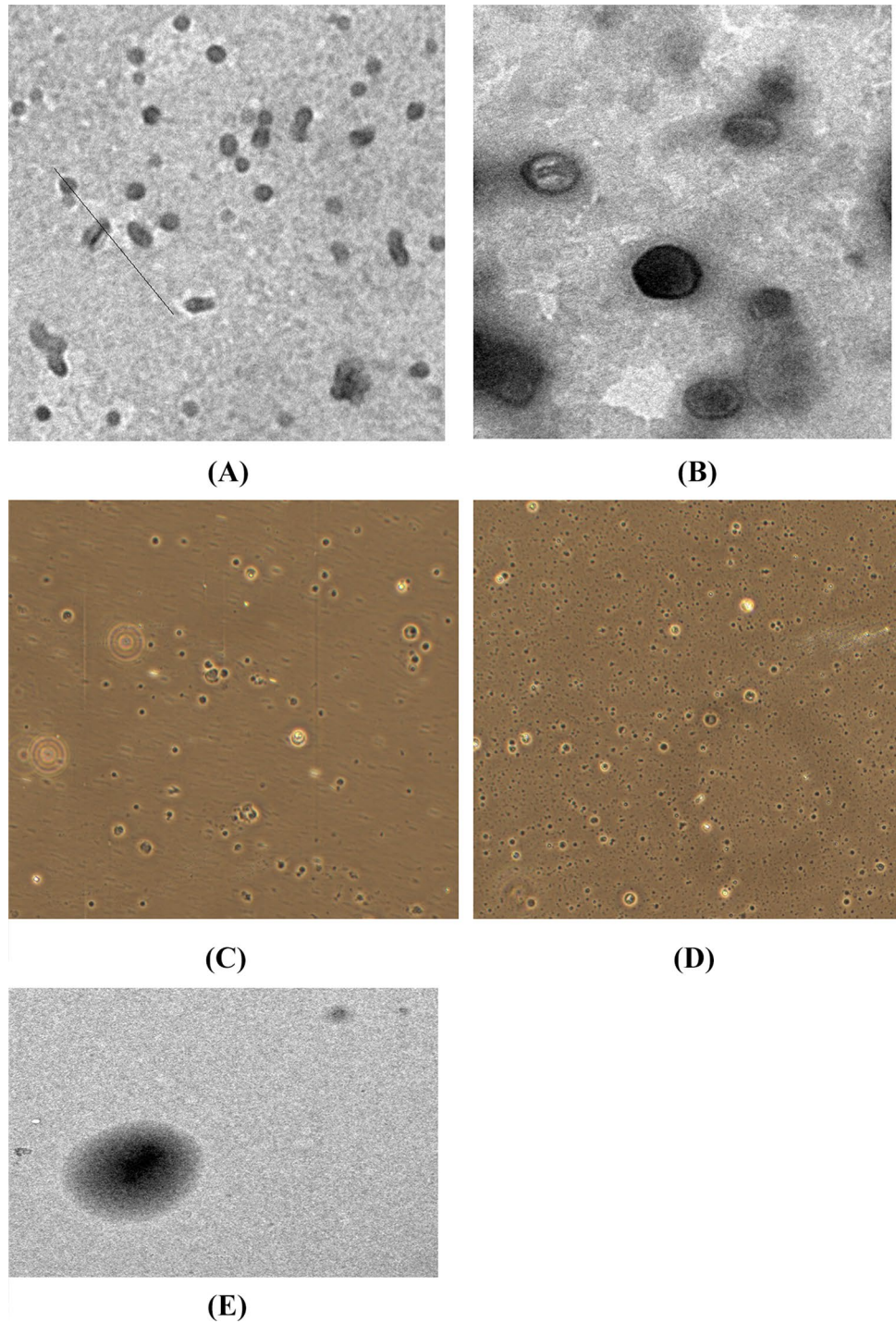
the lipophilic drug's entrapment within the core. It was found that the PDI values of the blank nanoparticulate systems were showing high heterogeneity in the given system, but on the encapsulation, the homogeneity was increased in the polydispersed phase. Zeta potential results showed that all the drug-loaded formulations are highly stable as the values are almost near ± 30 mV. The negative charge on the blank formulations may be due to the usage of phospholipid and other negatively charged components. This negative charge was further enhanced on the drug loading, which may be due to the negatively charged drug molecule [35]. For further verification, the microscopic analysis of the developed systems was performed and the microphotographs have been incorporated as Fig. 1. The results from the microscopic studies confirmed the formulation of the desired nanocarriers using the reported protocols.

### Evaluation Studies

#### In Vitro Drug Release Kinetics

The drug release profile of all the nanoformulations and the plain DTX in pH 7.4 and 5.6 are displayed in Fig. 2. The image clearly shows that the bag containing naïve DTX showed a high amount of release at physiological pH, i.e., pH 7.4 instead of cancer cell pH, i.e., pH 5.6. Notably, the release of DTX from the nanoformulations showed a controlled and pH-dependent pattern in a statistical manner ( $p < 0.05$ ). This feature helps in increasing the bioavailability of the drug at the tumor site and reduces the untoward biological responses resulting from higher doses. The rate of drug release was calculated and reported in Table 4 as the release flux values. The flux values also proved the statement of controlled drug releasing behavior of the developed nanoparticulate systems. By model fitting of the obtained drug release data, it was found that at pH 5.6, pure DTX, DTX-SLNs, DTX-NLCs, and DTX-ME followed the Higuchi model. DTX-LP and DTX-NIO followed zero and first-order release patterns. In pH 7.4, plain DTX, DTX-SLNs, and DTX-ME followed the Korsmeyer Peppas model. DTX-NLCs and DTX-LP followed the first-order pattern, whereas DTX-NIO showed the Higuchi release pattern [36]. The developed nanoparticulate systems were able to release the drug in both temporal and spatial pattern. This is the most desirable attribute in the delivery of the drug to the target site rather than its normal distribution to all the biological system.

**Fig. 1** The microphotographic images of SLNs (A), NLCs (B), liposomes (C), niosomes (D), and microemulsion (E)



### Blood Compatibility Studies

Figure 3 portrays the % hemolysis of naïve DTX and other drug-loaded nanoformulations. It was found that on the use of DTX-SLNs, DTX-NLCs, DTX-LP, DTX-NIO, and DTX-

ME, there was a significant 3.03, 2.42, 2.21, 3.46, and 2.69 fold decrease in the hemolysis in comparison to the pure DTX ( $p < 0.05$ ). This decrease can be ascribed to the entrapment of the drug molecules within the nanocarriers. From the image, it was evident that there was negligible hemolysis

**Fig. 2** Graphs showing % drug release of pure DTX, DTX-SLNs, DTX-NLCs, DTX-LP, DTX-NIO, and DTX-ME at (a) pH 5.6 and (b) pH 7.4, respectively, at t=24 h

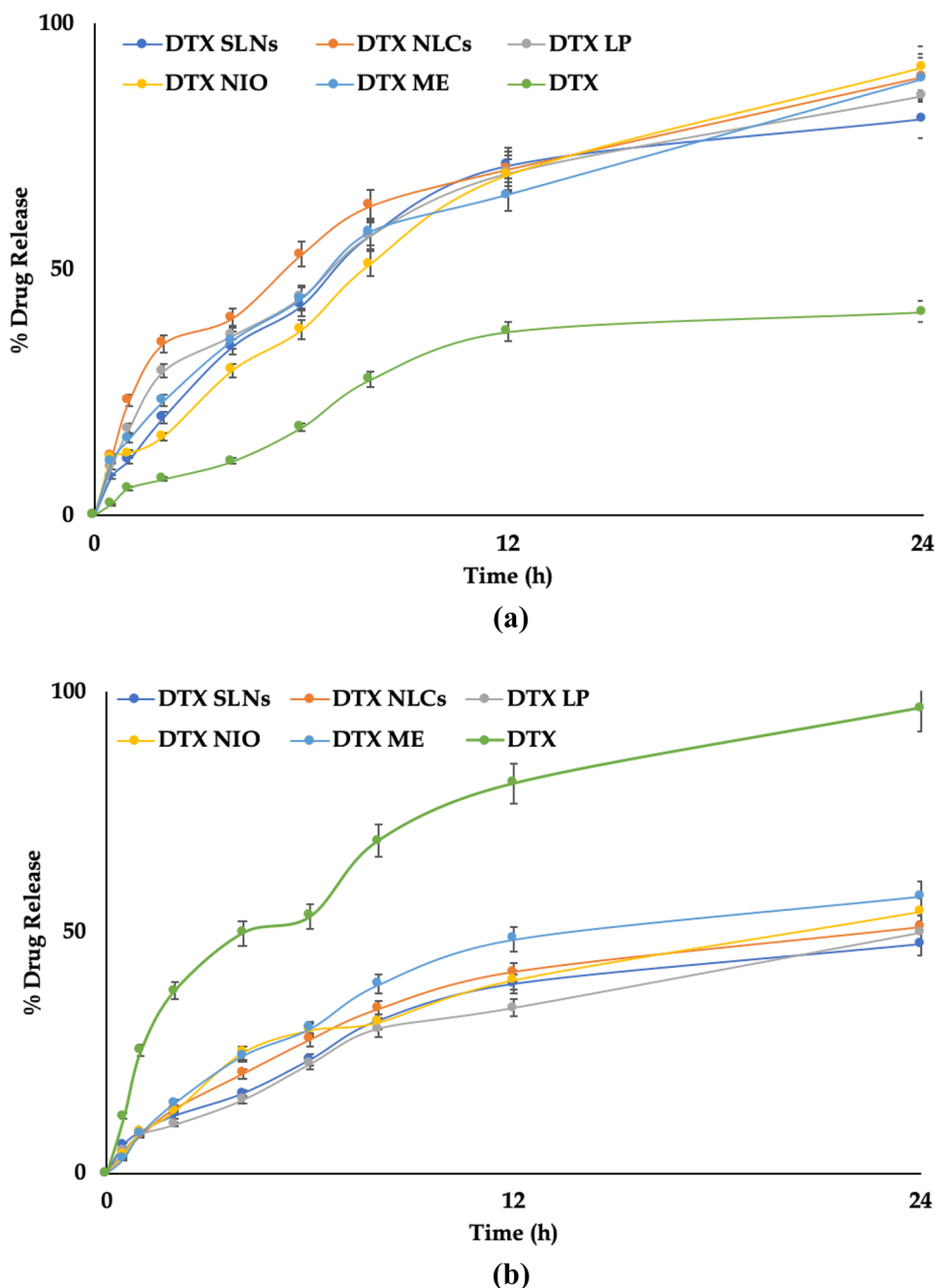


**Table 4** The values of average drug release flux plain DTX and nanoformulations at pH 5.6 and pH 7.4

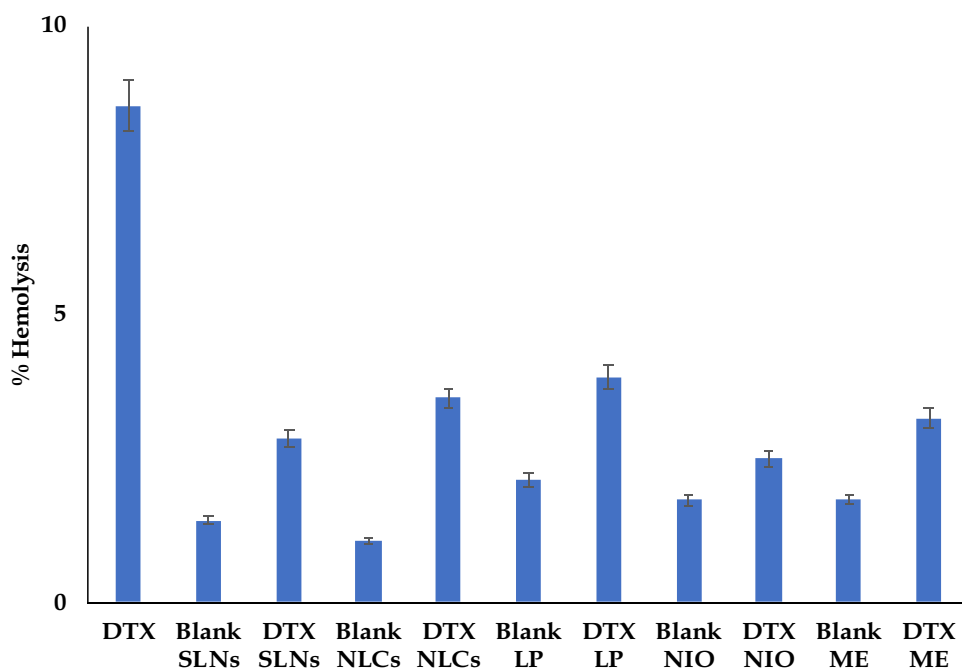
Nano formulations	Release flux values ( $\mu\text{g}/\text{h}/\text{cm}^2$ )	
	pH 5.6	pH 7.4
DTX	$1.72 \pm 0.29$	$4.03 \pm 0.57$
DTX-SLNs	$3.35 \pm 0.49$	$1.98 \pm 0.33$
DTX-NLCs	$3.72 \pm 0.56$	$2.13 \pm 0.35$
DTX-LP	$3.56 \pm 0.59$	$2.07 \pm 0.43$
DTX-NIO	$3.79 \pm 0.83$	$2.26 \pm 0.48$
DTX-ME	$3.69 \pm 0.67$	$2.40 \pm 0.38$

when the blank nanoformulations were evaluated, indicating the safety in using these carriers in the drug delivery. Henceforth, it can be concluded that developed nanosystems can be administered through an intravenous route due to their hemocompatible nature.

**Protein Binding Studies**

The amount of drug bound to the plasma proteins at various concentrations of pure drug and the nanoformulations is depicted in Fig. 4. A significant difference ( $p < 0.05$ )

**Fig. 3** Bar graph showing % hemolysis of pure DTX and developed nanoformulations



was observed between pure drug and the nanosystems in the protein binding of drugs. At every concentration, the amount of DTX bound from the nanoformulations was

lower than that of the naïve drug. It indicates that higher amount of drug will be available in the central compartment from the nanoparticulate systems than the plain drug.

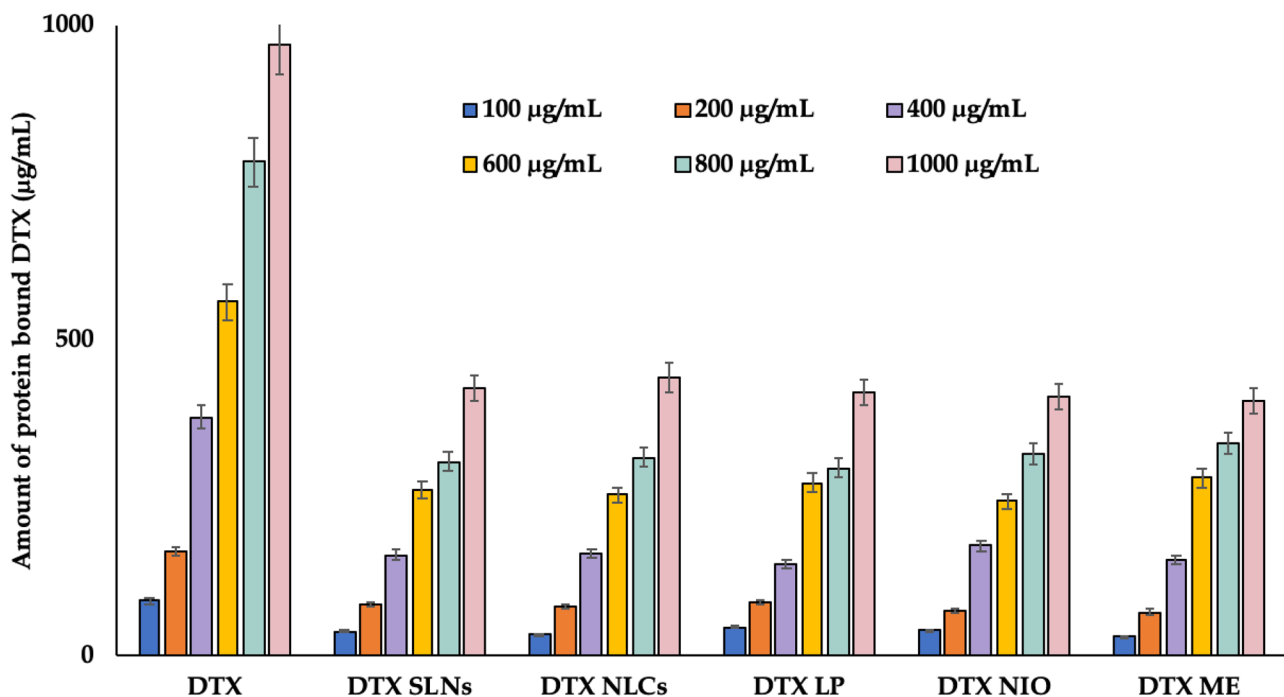


**Fig. 4** Figure depicting the variation in the bound drug to the plasma proteins at various concentrations of naïve DTX, DTX SLNs, DTX NLCs, DTX LP, DTX NIO, and DTX ME



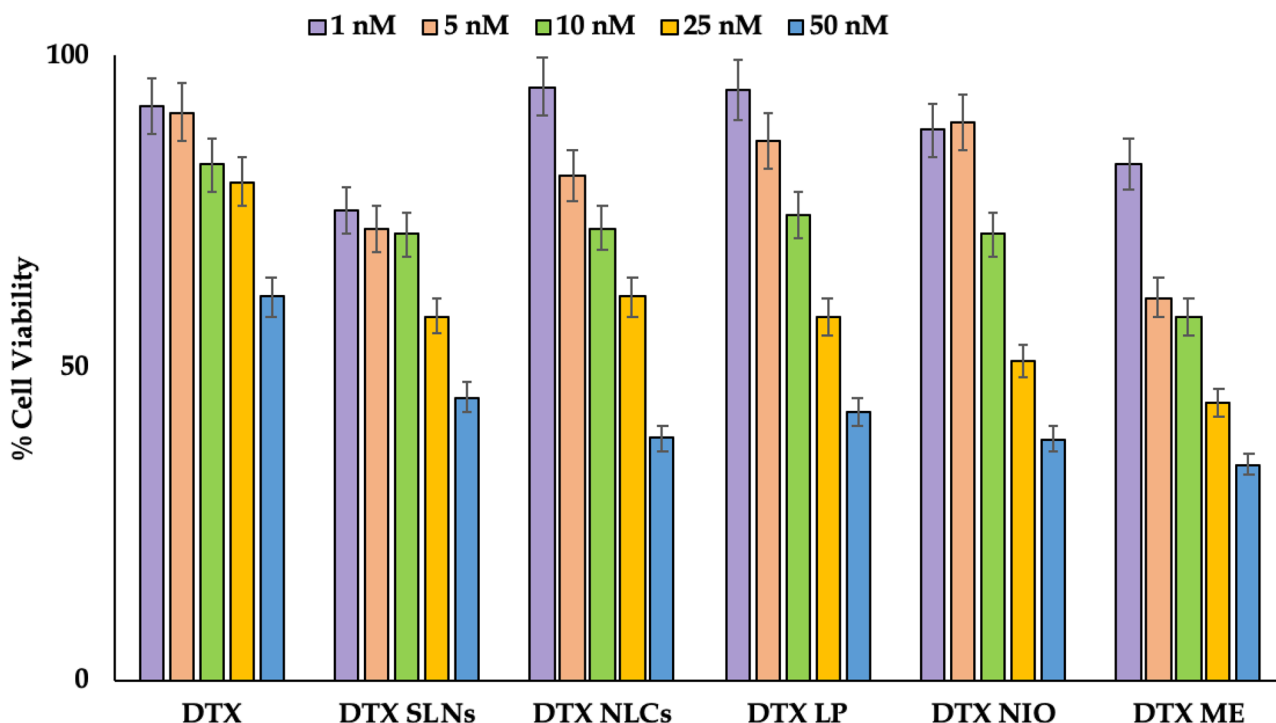


**Fig. 5** Bar graph showing % cell viability of pure DTX, DTX SLNs, DTX NLCs, DTX LP, DTX NIO, and DTX ME at various concentrations

The reduced protein binding helps increase the concentration of the drug, which will be available for the acting at the target site. This ultimately helps in decreasing the dosage along with the side effects caused during the treatment.

### Cell Studies

By treating the MDA-MB-231 cells with various concentrations of DTX and drug-loaded nanoformulations, % cell viability was evaluated, which is depicted as a bar diagram in Fig. 5.  $IC_{50}$  values of DTX, DTX-SLNs, DTX-NLCs, DTX-LP, DTX-NIO, and DTX-ME were found to be 77.12 nM, 22.61 nM, 35.07 nM, 40.52 nM, 32.81 nM, and 38 nM, respectively. A significant difference was observed between  $IC_{50}$  values ( $p < 0.05$ ). There was a statistical 3.44 (DTX-SLNs), 2.19 (DTX-NLCs), 1.90 (DTX-LP), 2.35 (DTX-NIO), and 2.02 (DTX-ME) fold decrease in the  $IC_{50}$  values, which indicates the increase in the potency of the drug ( $p < 0.05$ ). This change may be due to the specific release of the drug at the target site and helps reduce the side effects with enhanced efficacy. It was clearly evident that the nanoparticulate systems were able to penetrate the cells effectively and exert its effect in a better way

than the plain drug. The studies unequivocally vouched for the enhanced efficacy of the developed systems over its counterpart.

### Apoptosis Assay

Annexin V-FITC/PI assay was used to determine the apoptosis caused by the pure drug and other nanoformulations of MDA MB-231 cells. Figure 6 represents the flow cytometric data of the samples evaluated. In pure DTX, the apoptotic cells were 48.74% (37.65% early and 11.09% late), and the necrotic cell count was 1.05%. In DTX-SLNs, the apoptotic and necrotic cell count was 80.25% and 0%, respectively. DTX-NLCs showed 92.44% and 0.16% apoptosis and necrosis. DTX-LP exhibited 80.25% apoptosis and 0% necrosis. In the case of DTX-NIO, the % of apoptosis and necrosis was 91.33 and 0.94, respectively. DTX-ME showed 84.12% and 0.67% of apoptosis and necrosis. On statistical analysis, all the results were found to differ substantially at  $p < 0.05$ . It was evident that the nano-carriers induce a higher percentage of apoptosis. This may be due to increased permeability and cellular uptake rather than the pure DTX. The results showed the enhanced efficacy of the DTX on the encapsulation into nanocarriers. These findings are in close relation with the results of cell viability studies.

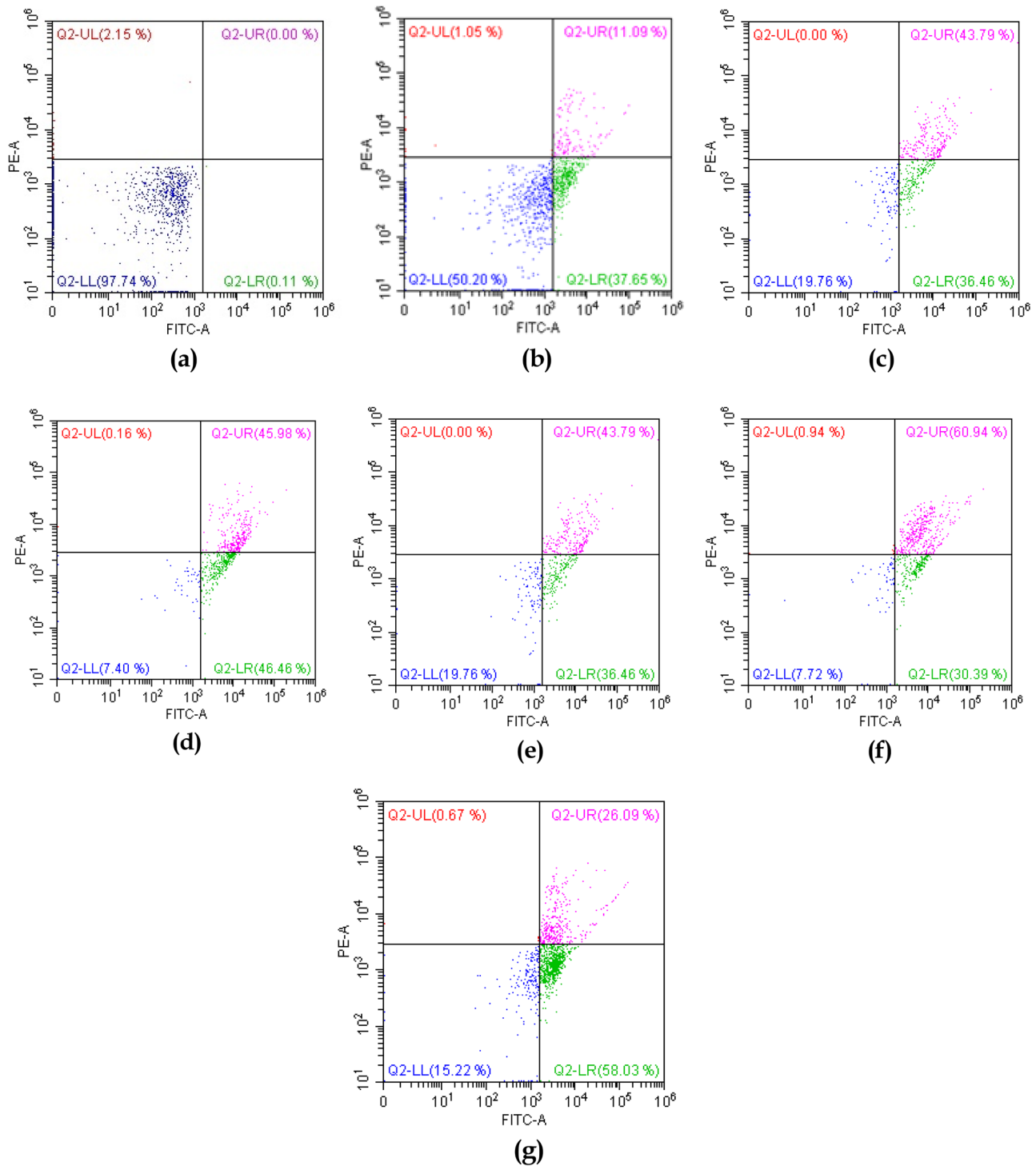


**Fig. 6** Pictorial representation showing apoptosis of **a** control, **b** DTX, **c** DTX SLNs, **d** DTX NLCs, **e** DTX LP, **f** DTX NIO, and **g** DTX ME

## Conclusion

After successful encapsulation of the DTX into the nanocarriers, there was enhanced anti-tumor activity and hemocompatibility. Through drug release studies, it was evident that the release was

in a controlled manner and pH-dependent. The protein binding of the drug was reduced drastically, which proves the availability of the drug to reach the target site. These carrier systems can offer a better pathway for delivering chemotherapeutic drugs belonging to BCS class IV, which have poor solubility and permeability.

**Acknowledgements** The lead author is thankful to the Deanship of Scientific Research (DSR) at Prince Sattam bin Abdulaziz University, under the research project number (2020/03/11935). M/s Fresenius Kabi India Pvt. Ltd., Gurgaon, Haryana, is also acknowledged for the generous gift sample of docetaxel.

## Declarations

**Conflict of Interest** The authors declare no competing interests.

## References

1. Farooq MA, Aquib M, Farooq A, Haleem Khan D, Joelle Maviah MB, Sied Filli M, Kesse S, Boakye-Yiadom KO, Mavlyanova R, Parveen A, Wang B. Recent progress in nanotechnology-based novel drug delivery systems in designing of cisplatin for cancer therapy: an overview. *Artif. Cells, Nanomedicine Biotechnol.* 2019. <https://doi.org/10.1080/21691401.2019.1604535>.
2. Mishra M, Kumar P, Rajawat JS, Malik R, Sharma G, Modgil A. Nanotechnology: revolutionizing the science of drug delivery. *Curr Pharm Des.* 2019;24:5086–107. <https://doi.org/10.2174/1381612825666190206222415>.
3. Raza K. Nanotechnology-based drug delivery products: need, design, pharmacokinetics and regulations. *Curr Pharm Des.* 2019;24:5085–5085. <https://doi.org/10.2174/138161282443190328085917>.
4. Safari J, Zarnegar Z. Advanced drug delivery systems: nanotechnology of health design A review. *J Saudi Chem Soc.* 2014. <https://doi.org/10.1016/j.jscs.2012.12.009>.
5. Jeevanandam J, Barhoum A, Chan YS, Dufresne A, Danquah MK. Review on nanoparticles and nanostructured materials: history, sources, toxicity and regulations. *Beilstein J. Nanotechnol.* 2018. <https://doi.org/10.3762/bjnano.9.98>.
6. Mir M, Ishtiaq S, Rabia S, Khatoon M, Zeb A, Khan GM, ur Rehman A, ud Din F. Nanotechnology: from in vivo imaging system to controlled drug delivery. *Nanoscale Res Lett.* 2017. <https://doi.org/10.1186/s11671-017-2249-8>.
7. Mohammadi MR, Nojoomi A, Mozafari M, Dubnika A, Inayathullah M, Rajadas J. Nanomaterials engineering for drug delivery: a hybridization approach. *J Mater Chem B.* 2017. <https://doi.org/10.1039/c6tb03247h>.
8. Singh R, Lillard JW. Nanoparticle-based targeted drug delivery. *Exp Mol Pathol.* 2009. <https://doi.org/10.1016/j.yexmp.2008.12.004>.
9. Ventola CL. Progress in nanomedicine: approved and investigational nanodrugs. *P T.* 2017;42:742–55.
10. Krishna VD, Wu K, Su D, Cheeran MCJ, Wang JP, Perez A. Nanotechnology: review of concepts and potential application of sensing platforms in food safety. *Food Microbiol.* 2018. <https://doi.org/10.1016/j.fm.2018.01.025>.
11. Sharma G, Thakur K, Raza K, Singh B, Katare OP. Nanostructured lipid carriers: a new paradigm in topical delivery for dermal and transdermal applications. *Crit Rev Ther Drug Carrier Syst.* 2017;34:355–86.
12. Jones S. Head-to-head: docetaxel challenges paclitaxel. *Eur J Cancer, Suppl.* 2006;4:4–8. [https://doi.org/10.1016/S1359-6349\(06\)80002-9](https://doi.org/10.1016/S1359-6349(06)80002-9).
13. Sohail MF, Rehman M, Sarwar HS, Naveed S, Salman O, Bukhari NI, Hussain I, Webster TJ, Shahnaz G. Advancements in the oral delivery of docetaxel: challenges, current state-of-the-art and future trends. *Int J Nanomedicine.* 2018. <https://doi.org/10.2147/IJN.S164518>.
14. Engels FK, Mathot RAA, Verweij J. Alternative drug formulations of docetaxel: a review. *Anticancer. Drugs.* 2007. <https://doi.org/10.1097/CAD.0b013e3280113338>.
15. Zhang E, Xing R, Liu S, Li P. Current advances in development of new docetaxel formulations. *Expert Opin Drug Deliv.* 2019. <https://doi.org/10.1080/17425247.2019.1583644>.
16. Zugazagoitia J, Guedes C, Ponce S, Ferrer I, Molina-Pinelo S, Paz-Ares L. Current challenges in cancer treatment. *Clin Ther.* 2016. <https://doi.org/10.1016/j.clinthera.2016.03.026>.
17. Kumar M, Sharma G, Misra C, Kumar R, Singh B, Katare OP, Raza K. N-desmethyl tamoxifen and quercetin-loaded multi-walled CNTs: a synergistic approach to overcome MDR in cancer cells. *Mater Sci Eng C.* 2018;89:274–82. <https://doi.org/10.1016/j.msec.2018.03.033>.
18. Kumar P, Sharma G, Gupta V, Kaur R, Thakur K, Malik R, Kumar A, Kaushal N, Raza K. Preclinical explorative assessment of dimethyl fumarate-based biocompatible nanolipoidal carriers for the management of multiple sclerosis ACS ChemNeurosci 2018;9. <https://doi.org/10.1021/acscchemneuro.7b00519>.
19. Kumar P, Sharma G, Kumar R, Malik R, Singh B, Katare OP, Raza K. Enhanced brain delivery of dimethyl fumarate employing tocopherol-acetate-based nanolipidic carriers: evidence from pharmacokinetic, biodistribution, and cellular uptake studies. *ACS Chem Neurosci.* 2017;8:860–5. <https://doi.org/10.1021/acscchemneuro.6b00428>.
20. Kumar P, Sharma G, Gupta V, Kaur R, Thakur K, Malik R, Kumar A, Kaushal N, Katare OP, Raza K. Oral delivery of methylthioadenosine to the brain employing solid lipid nanoparticles: pharmacokinetic, behavioral, and histopathological evidences. *AAPS PharmSciTech.* 2019;20:74. <https://doi.org/10.1208/s12249-019-1296-0>.
21. Wadhwa S, Singh B, Sharma G, Raza K, Katare OP. Liposomal fusidic acid as a potential delivery system: a new paradigm in the treatment of chronic plaque psoriasis. *Drug Deliv.* 2016;23:1204–13. <https://doi.org/10.3109/10717544.2015.1110845>.
22. Balasubramaniam A, Kumar VA, Pillai KS. Formulation and in vivo evaluation of niosome-encapsulated daunorubicin hydrochloride. *Drug Dev Ind Pharm.* 2002;28:1181–93. <https://doi.org/10.1081/DDC-120015351>.
23. Sharma G, Dhankar G, Thakur K, Raza K, Katare OP. Benzyl benzoate-loaded microemulsion for topical applications: enhanced dermatokinetic profile and better delivery promises. *AAPS PharmSciTech.* 2016;17:1221–31. <https://doi.org/10.1208/S12249-015-0464-0/TABLES/7>.
24. Raza K, Thotakura N, Kumar P, Joshi M, Bhushan S, Bhatia A, Kumar V, Malik R, Sharma G, Guru SK, Katare OP. C60-fullerenes for delivery of docetaxel to breast cancer cells: a promising approach for enhanced efficacy and better pharmacokinetic profile. *Int J Pharm.* 2015;495:551–9. <https://doi.org/10.1016/j.IJPHARM.2015.09.016>.
25. Thakur CK, Thotakura N, Kumar R, Kumar P, Singh B, Chitkara D, Raza K. Chitosan-modified PLGA polymeric nanocarriers with better delivery potential for tamoxifen. *Int J Biol Macromol.* 2016;93:381–9. <https://doi.org/10.1016/j.ijbiomac.2016.08.080>.
26. Du Y-Z, Lu P, Zhou J-P, Yuan H, Hu F-Q. Stearic acid grafted chitosan oligosaccharide micelle as a promising vector for gene delivery system: factors affecting the complexation. *Int J Pharm.* 2010;391:260–6. <https://doi.org/10.1016/j.ijpharm.2010.02.017>.
27. Kumar P, Sharma G, Kumar R, Malik R, Singh B, Katare OP, Raza K. Vitamin-derived nanolipoidal carriers for brain delivery of dimethyl fumarate: a novel approach with preclinical evidence. *ACS Chem. Neurosci.* acscchemneuro.7b00041. 2017. <https://doi.org/10.1021/acscchemneuro.7b00041>.
28. Misra C, Thotakura N, Kumar R, Singh B, Sharma G, Katare OP, Raza K. Improved cellular uptake, enhanced efficacy and promising pharmacokinetic profile of docetaxel employing glycine-tethered C60-fullerenes. *Mater Sci Eng C.* 2017;76:501–8. <https://doi.org/10.1016/j.msec.2017.03.073>.

29. Di Salle E, Pacifici GM, Morselli PL. Studies on plasma protein binding of carbamazepine. *Pharmacol Res Commun.* 1974;6:193–202. [https://doi.org/10.1016/S0031-6989\(74\)80028-7](https://doi.org/10.1016/S0031-6989(74)80028-7).
30. Thotakura N, Sharma G, Singh B, Kumar V, Raza K. Aspartic acid derivatized hydroxylated fullerenes as drug delivery vehicles for docetaxel: an explorative study. *Artif Cells, Nanomedicine, Biotechnol.* 2017;46:1–10. <https://doi.org/10.1080/21691401.2017.1392314>.
31. Date T, Nimbalkar V, Kamat J, Mittal A, Mahato RI, Chitkara D. Lipid-polymer hybrid nanocarriers for delivering cancer therapeutics. *J Control Release.* 2018;271:60–73. <https://doi.org/10.1016/j.jconrel.2017.12.016>.
32. Singh S, Chitkara D, Mehrazin R, Behrman SW, Wake RW, Mahato RI. Chemoresistance in prostate cancer cells is regulated by miRNAs and Hedgehog pathway. *PLoS ONE.* 2012;7:e40021. <https://doi.org/10.1371/journal.pone.0040021>.
33. Sharma S, Mazumdar S, Italiya KS, Date T, Mahato RI, Mittal A, Chitkara D. Cholesterol and Morpholine grafted cationic amphiphilic copolymers for miRNA-34a delivery. *Mol Pharm.* 2018;15:2391–402. <https://doi.org/10.1021/acs.molpharmaceut.8b00228>.
34. Thotakura N, Dadarwal M, Kumar P, Sharma G, Guru SK, Bhushan S, Raza K, Katare OP. Chitosan-stearic acid based polymeric micelles for the effective delivery of tamoxifen: cytotoxic and pharmacokinetic evaluation. *AAPS PharmSciTech.* 2017;18:759–68. <https://doi.org/10.1208/s12249-016-0563-6>.
35. Singh A, Thotakura N, Singh B, Lohan S, Negi P, Chitkara D, Raza K. Delivery of docetaxel to brain employing piperine-tagged PLGA-aspartic acid polymeric micelles: improved cytotoxic and pharmacokinetic profiles. *AAPS PharmSciTech.* 2019;20(220):1–10. <https://doi.org/10.1208/s12249-019-1426-8>.
36. Madhwi KR, Kumar P, Singh B, Sharma G, Katare OP, Raza K. In vivo pharmacokinetic studies and intracellular delivery of methotrexate by means of glycine-tethered PLGA-based polymeric micelles. *Int J Pharm.* 2017;519:138–44. <https://doi.org/10.1016/j.ijpharm.2017.01.021>.

**Publisher's Note** Springer Nature remains neutral with regard to jurisdictional claims in published maps and institutional affiliations.

Springer Nature or its licensor holds exclusive rights to this article under a publishing agreement with the author(s) or other rightsholder(s); author self-archiving of the accepted manuscript version of this article is solely governed by the terms of such publishing agreement and applicable law.

## Authors and Affiliations

Saad M. Alshahrani<sup>1</sup> · Nagarani Thotakura<sup>2</sup> · Saurabh Sharma<sup>3,4</sup> · Sheikh Shahnawaz Quadir<sup>2</sup> · Nishtha Chaurawal<sup>2</sup> · Sumit Sharma<sup>5</sup> · Deepak Chitkara<sup>4</sup> · Kaisar Raza<sup>2</sup> 

<sup>1</sup> Department of Pharmaceutics, College of Pharmacy, Prince Sattam Bin Abdulaziz University, Al-Kharj 11942, Saudi Arabia

<sup>2</sup> Department of Pharmacy, School of Chemical Sciences and Pharmacy, Central University of Rajasthan, Bandarsindri, Distt, Ajmer, Rajasthan 305 817, India

<sup>3</sup> Terasaki Institute for Biomedical Innovation, Los Angeles, CA 90064, USA

<sup>4</sup> Department of Pharmacy, Birla Institute of Technology and Science-Pilani (BITS), Pilani Campus, Vidya Vihar, Pilani, Rajasthan 333 031, India

<sup>5</sup> Delhi Pharmaceutical Sciences and Research University, New Delhi, India 110017